Investigation of structural, optical, and photocatalytic properties of hydrothermally synthesized ZnOnanorod arrays with various aspect ratios

Saeed Safa[1,*] , Ali Khayatian[2], Eliza Rokhsat[3], Mehrdad Najafi[4]

[1]*Young Researchers and Elite Club, South Tehran Branch, Islamic Azad University, Tehran, Iran*
[2]*Physics department, University of Kashan, Kashan, Iran.*
[3]*Plasma Physics Research Center, Science and Research branch, Islamic Azad University, Tehran, Iran*
[4]*Department of Physics, Shahrood University of Technology, Shahrood, Iran*

ARTICLE INFO

Article history:
Received 9 October 2015
Accepted 12 December 2015
Available online 20 January 2015

Keywords:
ZnOnanorod
Optical constant
Photocatalytic activity

ABSTRACT

Zinc oxide (ZnO) nanorods (NRs) with various aspect ratios (by changing the growth time between 0-240 min) were synthesized using hydrothermal method and were investigated using X-ray diffractometry (XRD), scanning electron microscopy (SEM) and UV–Visible and photoluminescence (Pl) spectroscopies. It was found that growth timeis directly related to the length, orientation and aspect ratio of the NR arrays.The optical transmittance of NR arrays indicated a regular decrement of average transmittance with increasing the length and aspect ratioof the NRs in the visiblerange. The porous ZnOnanorod grown for 240 min with the thickness of ~ 1.56 μm and texture coefficient of 0.96 exhibits some interesting properties like average visible transmittance of ~ 60%, refractive index of 1.34, packing density of 0.26 and lowest optical band gap. As the growth time increased, the PL intensity sustained a general weakening and a red-shift of UV-emission peak position. The UV-assisted photocatalytic degradation of 4-Nitrophenol (4-NP) of ZnO NRs were investigated. The considerable photocatalytic performance of ZnO NRs with highest aspect ratio was explained by its porosity and optical characteristics.

1. Introduction

Among the various optoelectronic materials, zinc oxide has been tremendously studied due to its wide band-gap energy (~3.37 eV), large exciton binding energy (~60 meV) and simple synthesis procedures [1-4]. These outstanding intrinsic properties have made the ZnO nanostructures as the most promising material for a wide range of uses in photonic crystals [1], transparent electrodes [2], ultraviolet (UV) light emitters [3], and photocatalyst applications [4]. In photocatalytic applications, ZnO acts as a sensitizer for light-induced redox interactions. More specifically, the photocatalytic chain reaction contains (i) co-generation of electrons and holes (e/h) in conduction and valence bands by photo-excitation; (ii) trapping the photoexcited electrons and holes by the surface groups to ultimately produce the hydroxyl radicals (-OH), which is known as the primary oxidizing species; and (iii) the hydroxyl radicals commonly mineralize the adsorbed organic substances [5]. However, bulk ZnO generally suffers from its negligible active surface area and wide band-gap.

Thus, some efforts have been made to regulate the photocatalytic properties of ZnO by changing its morphology [6] and doping by

* Corresponding Author:
E-mail Address: saeed.safa@modares.ac.ir

other additives [7]. Recently, Akhavan et al. [8] reported that ZnOnanorods (NRs) is the most favorable morphology for photocatalytic inactivation of *E. Coli* bacteria. More recently, Zhang et al. [9] synthesized high aspect ratio ZnO NRs on Zn foil and reported a remarkable photocatalytic efficiency and stability of ZnOnanorods compared to other similar works. Nevertheless, according to our knowledge, none of these researches have done a complete study on the relation between length and aspect ratio of ZnO NRs with optical characteristics and their natural extreme photocatalytic activity which is the main objective of this study. A number of studies have been published for controllable the growth of ZnO NRs, i.e. vapor-phase transport [10-12], pulsed laser deposition [13], chemical vapor deposition [14,15], electrochemical deposition [16], hydrothermal growth of nanorods [**Error! Bookmark not defined.**17-19], and molecular beam epitaxy [20]. Among the introduced methods, aqueous hydrothermal method has some advantages like its simplicity and low growth temperature, safety, cost-effectiveness. Thus, in this work, ZnO NR arrays with various aspect ratios (by changing the growth time) were synthesized in hydrothermal bath and their optical and structural characteristic were analyzed and compared. Afterwards, the photocatalytic performance of the samples was evaluated through degradation of 4-nitrophenol dye. In this study, 4-nitrophenol was selected as the model pollutant since it is a representative nitrophenol type contaminant and the most refractory pollutants, which can be present in industrial wastewater because of their high stability and solubility in water but little has been reported on its removal by ZnOnanorod arrays.

2. Experimental

2.1. Preparation of ZnO NRs

At first, microscopic glass slides were cleaned by acetone, ethanol and deionized water to remove the contaminants. Afterward, ZnO thin films were spin-coated onto each clean glass substrate to prepare the seed layer for NRs growth.

The spin-coating sol was prepared by a mixture of 0.05 M zinc acetate dihydrate and 0.06 M diethanolamine dissolved in ethanol. The solution was stirred at 60 °C for 20 min to become clear and homogeneous. Afterwards, the prepared sol was spin-coated onto the glass substrates at 3000 rpm for 30 sec. The coated films were dried at 180 °C for 10 min to evaporate the solvent and organic residuals. This procedure was repeated 5 times to produce a desired thickness of uniform ZnO films. Finally, the films were annealed at 500 °C for 1 h in air. Subsequently, after rinsing the ZnO seed layers by DI water, ZnO NRs were grown on the seed layers by suspending the samples in a super-saturated aqueous solution of 0.001 M zinc nitrate and 0.1 M sodium hydroxide at 70 °C for 20, 40, 60, 120 and 240 minutes. Then the samples were cleaned by deionized water to remove the residual salts and annealed at 500 °C for 1 h.

2.2. Characterization

The surface morphology of samples was depicted by scanning electron microscopy (SEM, VEGA, TESCAN). Also, due to the importance of seed layer topography and roughness for growth of NRs, the seed-layers were studied by atomic force microscope (AFM) using a Park Scientific model CP-Research (VEECO) apparatus. The structural characterization of samples was evaluated by X-ray diffractometry (XRD) using X'Pert PRO, Philips. The thickness of seed layer and NR thin films was evaluated by a thickness profilemeter using a Stylus-Dektak. Room temperature photoluminescence spectra (PL) were taken on a PL-Perkin-Elmer LS55 equipped with a 450W Xe lamp as the excitation source.

2.3. Photocatalytic study

In a typical process, the experiments were carried out through decolorization of a 5ppm 4-NitroPhenol (4-NP) solution with PH of 6. Prior to illumination, each sample was sank in solution for about 2 h in the dark to obtain adsorption-desorption equilibrium. Then, the samples were placed into the prepared solutions and were irradiated by a 400 W metal-halide lamp. Afterwards, the degradation was measured by taking out 3 ml aliquots at regular time intervals and monitoring their optical transmittance using a

double beam UV–Vis spectrophotometer at 400 nm wavelength.

3. Results and discussion

Fig. 1a shows the XRD patterns of ZnO NR arrays grown in 20, 60 and 240 min. The X-ray diffraction peaks of ZnO NRs grown for 20 min are not clear and only very weak peaks appear. Thus, to have a better depiction of the XRD peaks of NRs grown for 20 min, their XRD patterns were plotted individually in Fig. 2b. As can be seen in the inset of Fig. 1b, the peaks of the (100) and (002) planes are almost better distinguished.

The lack of any preferential orientation for this sample revealed that NRs are still in the initial stage of growth [21]. Although the diffraction peaks of the sample grown for 20 min are very weak, the 60 and 240 min grown samples show sharp peaks corresponding to the (100), (002), (101), (102) planes, indicating that both of the samples are crystallized in a preferential texture of hexagonal wurtzitestructure (JCPDS NO. 36-1451). Quantitative information concerning the preferential crystal orientation can be obtained from the texture coefficient, TC, defined as [18]

$$TC(hkl) = \frac{I(hkl)/I_0(hkl)}{(1/n)\sum_n I(hkl)/I_0(hkl)} \quad (1)$$

Where I(hkl) is the observed intensity of the (hkl) plane, I_0 (hkl) is the relative intensity of the corresponding plane given in the XRD reference (JCPDS 36-1451), and N is the total number of diffraction peaks. With increasing the growth time, the above-mentioned ratio (TC) increased considerably and estimated to be 0.14, 0.72 and 0.96 for NRs grown in 20, 60 and 240 min, respectively. Also, the mean crystallite size of the samples using the Scherrer equation [22] were obtained as ~19.01 , 22.24 and 39.82 nm for the ZnO NRs grown in 20, 60 and 240 min, respectively. It can be observed that with increasing the time of equilibrium growth of NRs in the hydrothermal bath, both the length of NRs toward the preferred orientation and the size of the crystallites increased. Moreover, as it was expected, the broad peak between 20°-35° originated from the amorphous glass substrate of the samples gradually disappeared by thickening of the ZnO NRs layer.

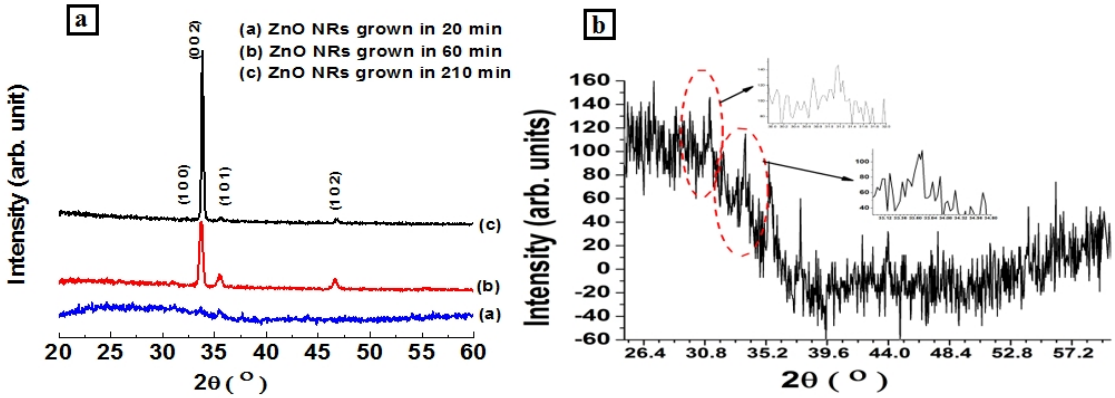

Fig 1.a) The X-ray diffraction patterns of ZnO NRs grown in hydrothermal bath for 20, 60 and 240min and b) magnified image of XRD patterns of ZnO NRs grown for 20 min. The inset shows locally magnified window of the (100) and (002) peaks for the sample grown for 20min.

The surface morphology of a seed film on glass substrate is shown by an AFM micrograph in Fig. 2. The seed layer appears to be a dense and almost without porosity film with average grain size ranging between 20 to 50 nm. The root mean square (RMS) surface roughness of the film was ~1.73 nm, indicating a nearly smooth and uniform layer for growth of NRs.

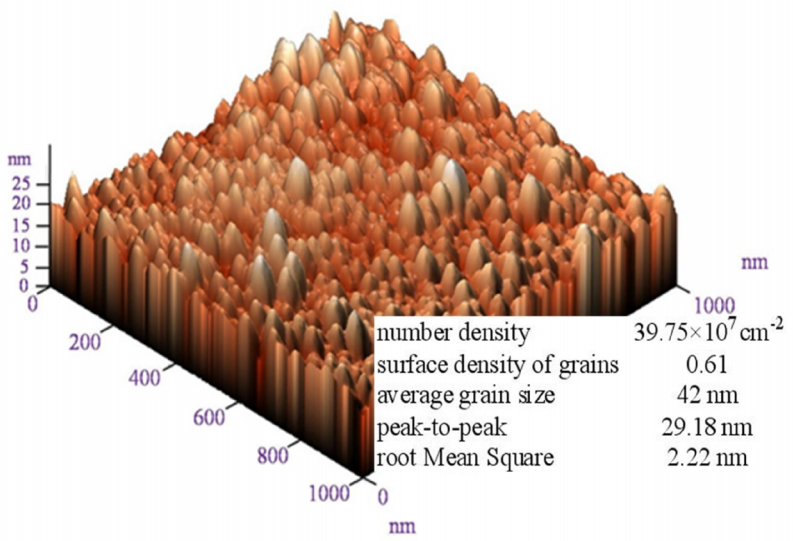

Fig 2. AFM microghraph of ZnO seed layer.

Fig. 3 shows the SEM image of the NR arrays grown at various times. Obviously, for the sample grown for 20 min, it is hard to talk about the formation of ZnOnanorods. In fact, some occasional nano-features are seen in the image. It means that under the applied conditions for hydrothermal growth, the NRs are in the initial states for crystallization and growth (in good agreement with the XRD results).

With increasing the time of growth to 60 min, a close-packed array of NRs with an average diameter of ~ 80 nm is formed. Moreover, the SEM image of ZnO arrays shows that the growth direction of NRs is nearly toward the normal direction of substrate. The growth mechanism of ZnO NRs in aqueous solution is based on heterogeneous nucleation and subsequent crystal growth on the seed layer. During the hydrothermal growth, an equilibrium point between the precipitation and etching reactions between supersaturated $Zn(NO_3)^{-2}$ and ZnO coated seed layer is established. In this state, $Zn(NO_3)_2$ hydrolyses in alkaline solution and forms the complexion $[Zn(OH)_n]_{2-n}$ (n = 2 or 4). Predominantly, the following reactions have been proposed for ZnOnanorods precipitation [8]:

$$2[Zn(OH)_n]^{2-n} \rightarrow [Zn_2O(OH)_{2n-2}]^{4-2n} + H_2O$$

With increasing the temperature up to 70 °C, the complexes dehydrate [i] on the surface of growing crystals which results in the heterogeneous growth at the interface between the substrate and solution especially along the most closely-pack direction [0001] with the lowest energy planes [ii,25]. Accordingly, it could be seen that with increasing the growth time, the average NRs diameter obtained from SEM images increases a little from ~ 80 nm to ~ 100 nm for NRs grown in 60 and 240 min, respectively, while the lengths of NRs obtained from Dektak were estimated ~ 85 nm, 353 nm, 895 nm, 1.25 µm and 1.56 µm for 20, 40, 60, 120 and 240 min grown ZnO NR samples, respectively. Therefore, one can conclude that the (002) plane is preferentially grown rather than any other planes. In this regard, Abbasi et al. [iii] suggested that nitrate anions facilitate the preferential growth of high energy (002) plane toward [0001] direction of ZnO unit cell in an alkaline growth solution.

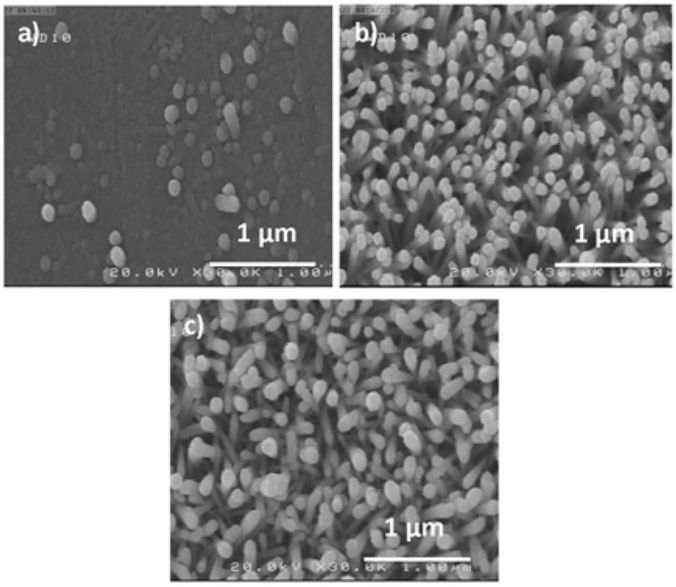

Fig 3. the SEM images of NR films grown in hydrothermal bath for a) 20, b) 60 and c) 240 min.

Fig. 4 shows the room temperature photoluminescence (PL) spectra of ZnO NR films grown for 20, 60 and 240 min. To evaluate and compare the photoluminescence of each sample, the emission spectra were deconvoluted by Gaussian function to the four distinct peaks. The sharp peaks at ~402 nm are assigned to UV-emission due to recombination of free excitons. The visible emissions at ~467 and 522 nm (blue and green emissions) mainly originates from the different defect states such as existence of Zn-interstitials and O-vacancies in lattice structure of ZnO. The broad emission band between 400-700 nm observed in all samples is assigned to deep level emission band (DLE) [iv]. It can be observed that the intensity of PL peaks decreased and UV-emission peak position is red-shifted from (λ = 397.5 nm, Intensity = 75.5 arb. u.) to (λ= 410.3 nm and Intensity = 8.66 arb. u.) with the increase of NR films thickness. The UV-emisson red-shift could be explained by the regular multi-dispersity of incident light among the prolonged ZnOnanorods. The same observations are made in optical absorption and also edge of absorption (as optical band gap) . Moreover, the increment of the defect induced peak to free exciton peak for NRs with higher aspect ratio (or length) could be due to an increased number of surface states occupied by lattice defects for longer NRs [v].

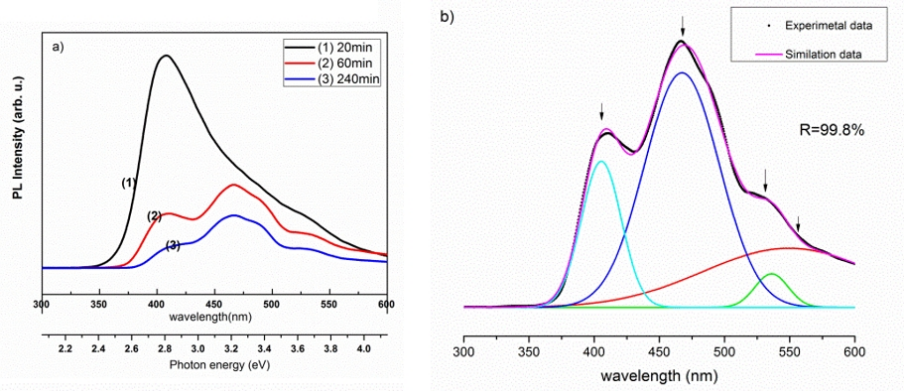

Fig 4.a) Photoluminescence spectra of hydrothermally grown ZnOnanorods for various time of growth measured at room temperature and b) deconvolution of the PL spectrum of ZnOnanorods grown for 60 min in hydrothermal bath.

The transmittance and reflectance spectra of ZnO seed and NR films in the range of UV-Vis are shown in Fig. 5a,b. The transmittance of the seed sample is about 90% while it decreases to about 60% for ZnO NRs grown for 240 min. The decrement of optical transmittance is associated with light scattering and absorption by the surface of NRs [vi-vii].

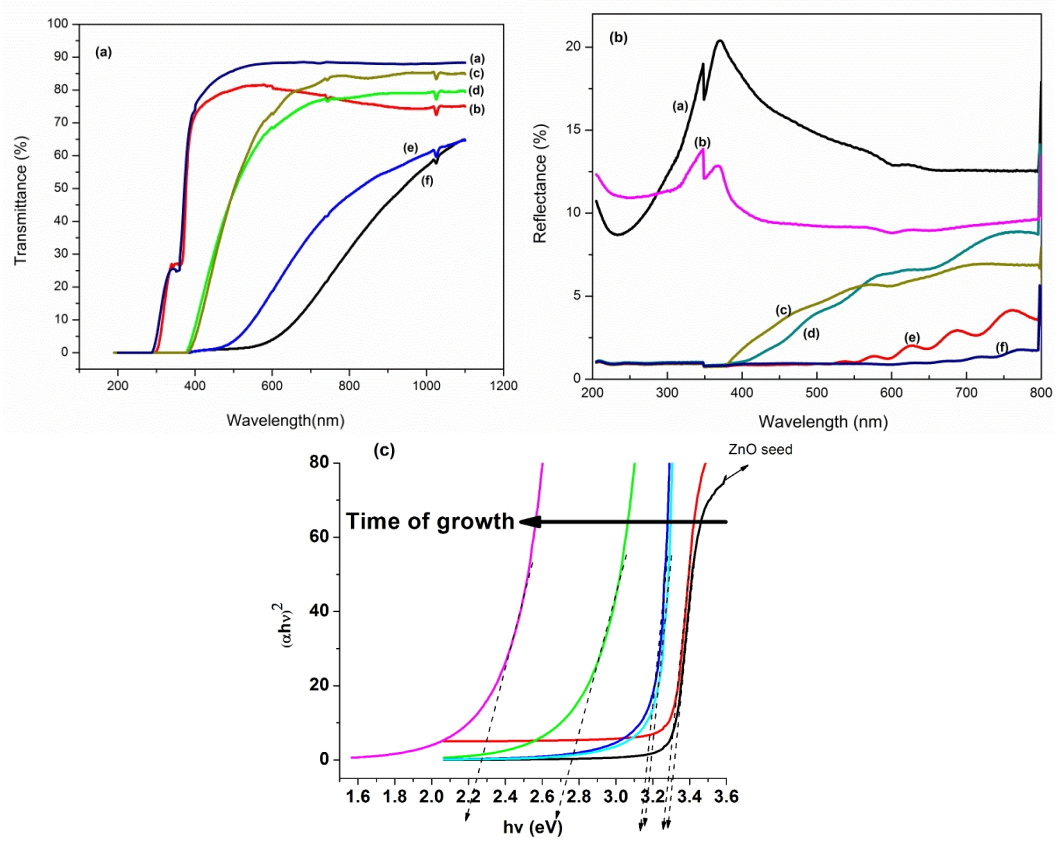

Fig 5. Optical transmittance and reflectance spectra of ZnO a) seed layer, and hydrothermally synthesized NRs grown for b) 20, c) 40, d) 60, e) 120 and f) 240 min.

Using the optical spectra, one can evaluate the band gap energy (E_g) of the samples. At first, the optical density (defined as the product of the absorption coefficient and thickness of the film) can be evaluated as $\alpha t = \ln(100/T)$ in which α, t, and T are the absorption coefficient, thickness and transmittance of the film, respectively. The optical density is utilized to obtain E_g of the thin films by plotting the curve of$(\alpha h\nu)1/\eta$ versus hν for the relation $\alpha h\nu = A(h\nu - E_g)^{\eta}$ where A is a constant and η is another constant which depends on the nature of the transition. For the ZnO-based materials, it is assumed that $\eta = 1/2$ corresponding to the direct allowed electron transition mechanism. Therefore, just at the beginning of the absorption region (hν ~ Eg) where the plot of $(\alpha h\nu)^2$ versus hν shows a linear behavior, the intercept of the extrapolated fitted line with the hν axis gives the optical band gap energy. Fig. 5c shows the graphical presentation of $(\alpha h\nu)^2$ versus the incident photon energy (hν). The band gap energy of the bare ZnO thin film was found to be about 3.3 eV which is consistent with the band gap energy usually reported for bulk ZnO (3.2 eV). It can be seen that by increasing the length of ZnOnanorods, the value of Eg decreases from ~3.3 to ~2.1 eV. Therefore, ZnOnanorods grown in prolonged times appropriately absorb the visible light irradiation. The decrease in the band gap can be attributed to the multiple scattering and absorption of incident wavelength between lengthy nanorods (see Fig.7).

Concerning the thickness of ZnO NRs measured by Dektak, the absorption coefficient can be obtained by the following formula [viii]:

$$\alpha = \frac{\ln(\frac{(1-R)^2}{T})}{d} \quad (2)$$

The sharp absorption edge of ZnO seed sample observed at ~380 nm is very close to the intrinsic band gap of bulk ZnO (3.37 eV).

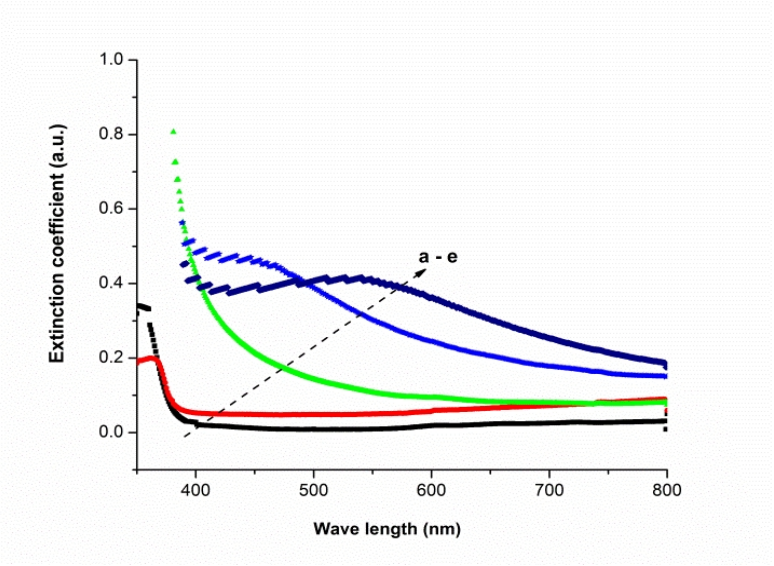

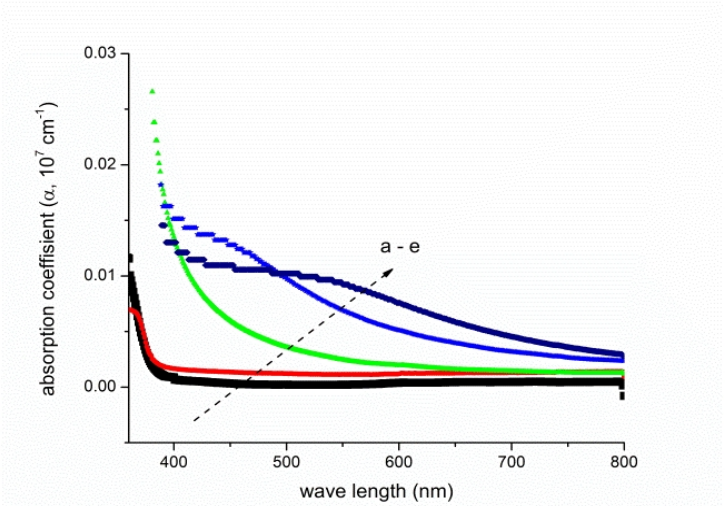

Fig 6. The calculated absorbance and extinction coefficient of ZnO a) seed and NR thin films grown in b) 20, c) 60, d) 120 and e) 240 min of hydrothermal bath.

The incident light can pass through the lateral surfaces of the rods, and multiple scattering of UV among those gaps may occur, as schematically shown in Fig. 7. Therefore, the regular increment of absorption coefficient could be explained by higher poly-dispersity of UV and/or visible emissions with increasing the length of NRs [28].

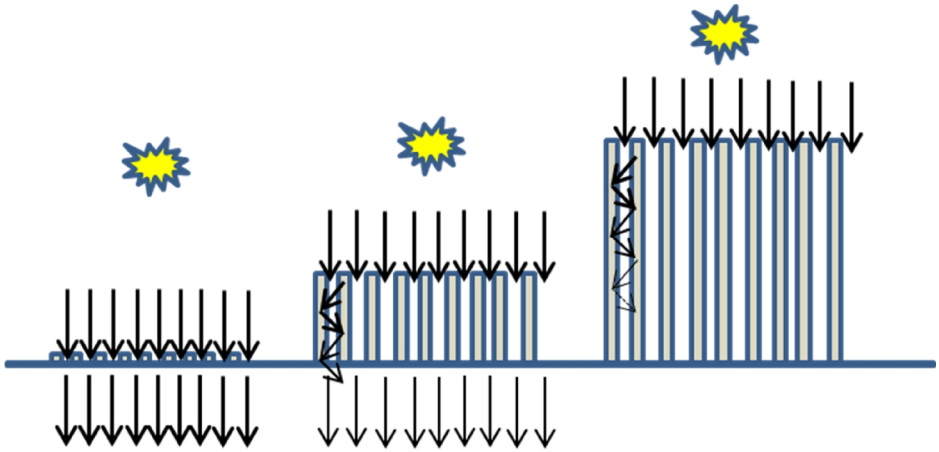

Fig 7. Schematic of incident light interaction with ZnOnanorod samples with various length.

Using the values of the absorption coefficients, calculated by the above mentioned formulas, the extinction coefficient can be obtained from below relation:

$$k = \frac{\alpha\lambda}{4\pi} \quad (3)$$

The calculated extinction coefficient of ZnO seed and NRs is shown in Fig. 5. The extinction coefficient of the seed layer is negligible (near to zero), while it increased by the growth of NRs. The refractive index of the ZnO seed and NR films were calculated by the following relation:

$$n = \frac{1+R}{1-R} + \sqrt{\frac{4R}{(1-R)^2} - k^2} \quad (4)$$

Where n is the refractive index and k is extinction coefficient. It is worth noting that the refractive index changes sharply near the optical absorption edge and then tends to be constant in the visible region [ix]. Therefore, the refractive index was calculated at the typical wavelength of 600 nm for all samples and summarized in Table 1. The refractive index of ZnO seed layer was calculated to be ~2.01 which is in close agreement with the literature [x]. Also, the refractive index of the NR films decrease with increasing the growth time. In this regard, it is suggested that the reduction of the refractive indices with growing the length of NRs could be mainly attributed to the increment of absorption coefficient [xi]. In order to evaluate the extent of inter-columnar volume and voids between ZnO NRs, the porosity of the films is calculated using Lorentz–Lorentz equation [xii]:

$$p = 1 - \left[\frac{[(n_f^2 - 1)/(n_f^2 + 2)]}{[(n_s^2 - 1)/(n_s^2 + 2)]}\right] \quad (5)$$

Where n_f is the refractive index of the ZnO NR films and n_s is the refractive index of a dense ZnO thin film which is widely accepted to be 2. It is clear that the porosity of the analyzed films increased considerably by increasing the length of NRs which could be the rational result of NRs growth [it is supported by SEM photographs, Figs. 3 and XRD pattern, Fig. 1].

Table 1. The refractive index, calculated porosity and photocatalytic kinetic constant of ZnO seed and NRs grown in various time of hydrothermal bath.

Growth time	0 (Seed sample)	20	40	60	120	240
Refractive index (at $\lambda = 600nm$)	2.01	1.9	-	1.7	1.4	1.3
porosity	1	0.07	-	0.23	0.51	0.74
k (h^{-1})	0.05	0.069	0.16	0.18	0.33	0.30

For comparison, Moustaghfir et al.[2] reported the refractive index (at λ=633 nm) and porosity of the radio frequency magnetron sputtered ZnO film (with thickness of ~800

nm) 1.89 and 0.07, respectively, which is in close agreement with our results.

The photocatalytic activities of all samples were compared by measuring 4-NP solution decolorization under light irradiation. The typical degradation of 4-NP molecules for ZnO NRs grown for 240 min is shown in Fig. 8.

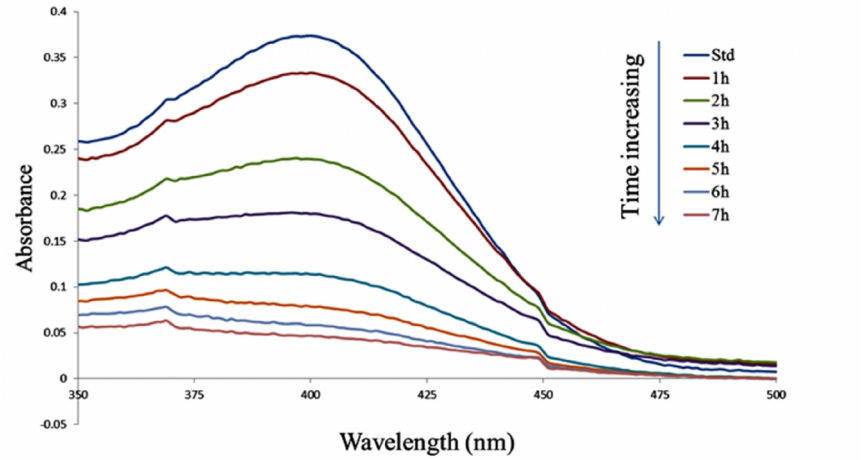

Fig 8. The typical 4-NP photocatalyticaldecolorization using 240 min grown ZnO NRs as catalyst.

To estimate and compare the photocatalytic performance of ZnO seed and NRs, the absorption values at λ=400 nm were measured (Fig. 9). Moreover, it was found that the photodegradation reaction of 4-NP by ZnO NRs follows from pseudo-first-order kinetic model. The extracted kinetic constants from this model for all samples are summarized in Table 1.

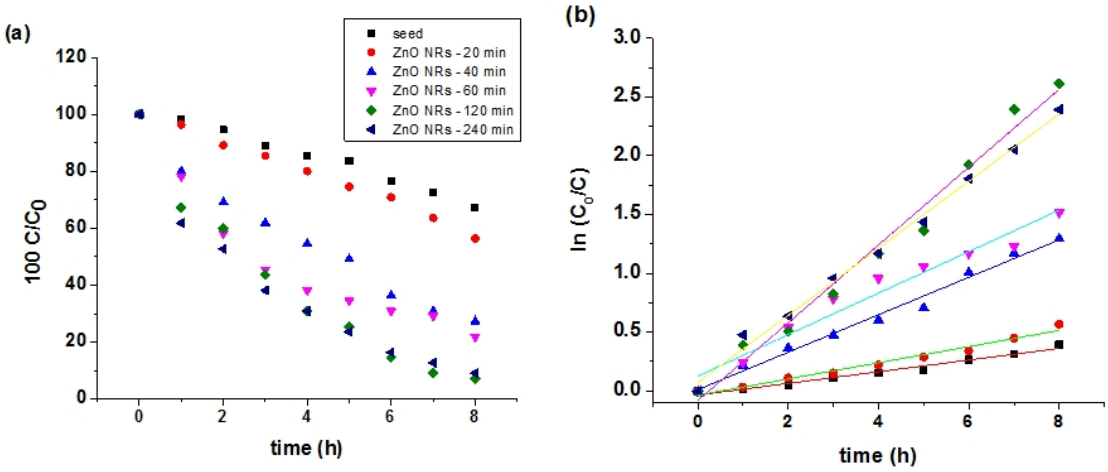

Fig 9.a) photocatalytic degradation and b) corresponding kinetic constant rate modeled by pseudo-first-order of 4-NP by ZnO seed and NRs.

It is clear that among the samples, the ZnO NRs grown for 120 and 240 min show the highest photocatalytic activity under UV/Visible light (metal-halide light source). This can be explained by three main reasons; 1) the optical absorption and correspondingly extinction coefficient of ZnO NRs is extended in the visible light range with increasing the NRs length, 2) the PL UV-emission band which is related to the recombination of electron/hole pairs decreased considerably [38] and 3) higher porosity (calculated from

refractive index) and subsequently higher surface effective area of prolong grown ZnO NRs [39].

4. Conclusions

This work provides a systematic study on the growth of ZnOnanorod arrays by hydrothermal method. It was observed that nitrate anions cause the preferential growth of ZnO crystals toward [0001] direction in alkaline hydrothermal bath. The crystallite size was found to be increased from ~19.01 to 39.82 nm with increasing the growth time from 20 to 240 min. The optical results also showed that with increasing the length of NRs, the absorption coefficient decreased and red-shifted. The simultaneous decrement of PL near the band gap emission, red-shift of the optical edge of absorption and higher calculated porosity show an optimized state for photocatalytic performance of ZnO NRs with longer length.

References

[1] Janotti, C. G. Van de Walle, Fundamentals of zinc oxide as a semiconductor, Rep. Prog.Phys. 2009, **72**, 126501.

[2] V. Srikant, V. Sergo, D. R. Clarke, Epitaxial Aluminum-Doped Zinc Oxide Thin Films onSapphire: I, Effect of Substrate Orientation, J. Am, Ceram. Soc. 1995, **78**, 1931-1934.

[3] Y. Ryu, T.-S. Lee, J. A. Lubguban, H. W. White, B.-J. Kim, Y.-S. Park, C.-J. Youn, Next generation of oxide photonic devices: ZnO-basedultraviolet light emitting diodes, Applied Physics Letters, 2006, **88**, 241108-241108.

[4] H. Fu, T. Xu, S. Zhu, Y. Zhu, Photocorrosion inhibition andenhancement of photocatalytic activity for ZnO via hybridization with C60, Environ. Sci.Technol. 2008, **21**, 8064.

[5] C. Ren, C. Beifang, Y. Min, Wu, J. Xu, Z. Fu, T. Guo, Y. Zhao,C. Zhu, Synthesis of Ag/ZnOnanorods array with enhanced photocatalyticperformance, J. Hazard. Mater. 2010, **182**, 123.

[6] Y. Liu, H. Lv, S. Li, X. Xing, G. Xi, Preparation and photocatalytic property of hexagonal cylinder-like bipods ZnO microcrystal photocatalyst, Dyes and Pigments, 2012, **95**, 443-449.

[7] J.H. Bang, S. Kenneth, Applications of ultrasound to the synthesis of nanostructured materials, Advanced Materials, 2010, **22**, 1039-1059.

[8] O. Akhavan, M. Mehrabian, K. Mirabbaszadeh, R. Azimirad, Hydrothermal synthesis of ZnOnanorod arrays for photocatalytic inactivation of bacteria, J. Phys. D: Appl. Phys. 2009, **22**,225-305.

[9] J. Zhang, Y. Su, H. Wei, J. Wang, C. Zhang, J. Zhao, Z. Yang, M. Xu, L. Zhang, Y. Zhang,Double-nucleation hydrothermal growth of dense and large-scale ZnOnanorod arrays with highaspect ratio on zinc substrate for stable photocatalytic property, Mater. Lett. 2013, **107**, 251.

[10] W. Park, D. Hl Kim, S-W. Jung, Gyu-Chul Yi, Metalorganic vapor-phaseepitaxial growth of vertically well-aligned ZnOnanorods, Applied Physics Letters, 2002, **80**, 4232.

[11] Q. X. Zhao, P. Klason, M. Willander, Growth of nanostructures by vaporliquidsolidmethod,Appl. Phys. A, 2007, **88**, 27-30.

[12] M. H. Huang, Y. Wu, H. Feick, N. Tran, E .Weber, P. Yang, Catalytic Growth of ZincOxide Nanowires by Vapor Transport, Adv. Mater., 2001, **13**, 113-116.

[13] x. Sun, G. M. Fuge, M. N. R. Ashfold, Growth of aligned ZnOnanorods arrays bycatalysis-free pulsed laser deposition methods, Chem. Phys. Lett. 2004, **396**, 21-26.

[14] J.Wu, S. C. Liu, Low-Temperature Growth of Well-Aligned ZnONanorods by ChemicalVapor Deposition, Adv .Mater., 2002, **14,** 215-218.

[15] W. I. Park, D. H. Kim, S.W. Jung G. C. Yi, Metalorganic vapor-phase epitaxial growth ofvertically well aligned ZnOnanorods, Appl. Phys. Lett., 2002, 80, 4232-4234.

[16] H. D. Yu, Z. P. Zhang, M. Y. Han, X. T. Hao, F. R. Zhu, A general low-temperatureroute for large-scale fabrication of highly oriented ZnOnanorod/nanotube arrays, J. Am. Chem.Soc. 2005**, 127**, 2378-2379.

[17] J. X. Wang, X. W. Sun, Y. Yang, H. Huang, Y. C. Lee, O. K. Tan, L. Vayssieres,Hydrothermally grown oriented ZnOnanorod arrays for gas sensing applications, Nanotech. 2006, **19**, 4995.

[18] A. Wei, X.W. Sun, J. X. Wang, Y. Lei, X. P. Cai, Chang Ming Li, Z. L. Dong, W. Huang,Enzymatic glucose biosensor based on ZnOnanorod array grown by hydrothermaldecomposition, Appl. Phys. Lett. 2006, **12,** 123902.

[19] M. Guo, P. Diao, S. Cai, Hydrothermal growth of well-aligned ZnOnanorodarrays: Dependence of morphology and alignment ordering upon preparing conditions, SolidState Chem. 2005, 178, 1864.

[20] A. Bakin, A. El-Shaer, A. CheMofor, M. Kreye, A. Waag, F. Bertram, J. Christen, M.Heuken, J. Stoimenos, MBE growth of ZnO layers on sapphire employing hydrogen peroxide asan oxidant, J. Cryst. Growth, 2006, **287**, 7-11.

[21] O. Akhavan, R. Azimirad, S. Safa, M. M. Larijani, Visible light photo-induced antibacterialactivity of CNT–doped TiO2 thin films with various CNT contents, J. Mater. Chem. 2010, **20**,7386.

[22] B.D. Cullity, "X-ray Diffraction." Addison-Wesley Publishing Company, 1956, **204**, 158-159.

[23] O. Akhavan, M. Mehrabian, K. Mirabbaszadeh, R. Azimirad, Hydrothermal synthesis ofZnOnanorod arrays for photocatalytic inactivation of bacteria, J. Phys. D: Appl. Phys. 2009, **42**, 225305.

[24] M. Breedon, C. Rix, K. Kalantar-zadeh, Seeded Growth of ZnONanorods from NaOHSolutions, Mater.Lett. 2009, **63**, 249-251.

[25] M.A. Abbasi, Y. Khan, S. Hussain, O. Nur, M. Willander, Anions effect on the lowtemperature growth of ZnO nanostructures, Vacuum, 2012, **86**, 1998-2001.

[26] B. J. Lawrie, R. F. Haglund, R. Mu, Enhancement of ZnO photoluminescence by localizedand propagating surface plasmons, Opt. Express, 2009, **17**, 2565-2572.

[27] Y.G. Wang, S.P. Lau, H.W. Lee, S.F. Yu, B.K. Tay, X.H. Zhang, H.H. Hng,Photoluminescence study of ZnO films prepared by thermal oxidation of Zn metallic films in air,J. Appl. Phys., 2003, **94**, 354–358.

[28] R.N. Gayen, R. Bhar, A.K. Pal, Synthesis and characterization of vertically aligned ZnOnanorods with controlled aspect ratio, Indian J. pure and appl. Phys., 2010, **48**, 385-393.

[29] G.Srinivasan, J.Kumar, Effect of Mn doping on the microstructures and optical properties ofsol-gel derived ZnO thin films , J. Cryst. Growth, 2008, **310**, 1841–1846.

[30] L. Xu, X. Li, J. Yuan, Effect of K-doping on structural and optical properties of ZnO thinfilms, SuperlatticesMicrostruct., 2008, **44**, 276-281.

[31] M. Vishwas, K. Narasimha Rao, K. V. Gowda, R. P. S. Chakradhar, Effect of sintering onoptical, structural and photoluminescence properties of ZnO thin films prepared by sol–gelprocess, Spectrochim. Acta, Part A. 2010, **77**, 330-333.

[32] H. C. Genuino, D. T. Horvath, C. K. King'ondu, G. E. Hoag, J. B. Collins, Steven L. Suib, Effects of visible and UV light on the characteristics and properties of crude oil-in-water (O/W) emulsions, Photochemical &Photobiological Sciences, 2012, **11**, 692-702.

[33] S.W. Xue, X.T. Zu, W.G. Zheng, H.X. Deng, X. Xiang, Effects of Al doping concentrationon optical parameters of ZnO:Al thin films by sol–gel technique, Physica B, 2006, **381**, 209–213.

[34] S. Ilican, Y. Caglar, M. Caglar, F. Yakuphanoglu, Structural, optical and electricalproperties of F-doped ZnOnanorod semiconductor thin films deposited by sol–gel process.Appl. Surf. Sci., 2008, **255**, 2353–2359.

[35] M. Naser, S. Zaliman, Al-DouriYarub, “Investigation of the absorption coefficient,refractive index, energy band gap, and film thickness for Al0. 11Ga0. 89N, Al0. 03Ga0. 97N,and GaN by optical transmission method”, International Journal of Nanoelectronics andMaterials, 2009, **2**, 189-195.

[36] M. Dutta, S. Maridha, D. Basak, Effect of sol concentration on the properties of

ZnO thinfilms prepared by sol–gel technique Appl. Surf. Sci., 2008, **254**, 2743–2747.

[37] A. Moustaghfir, E. Tomasella, S.B. Amor, M. Jacquet, J. Cellier, T. Sauvaget, Structuraland optical studies of ZnO thin films deposited by rf magnetron sputtering: influence ofannealing, Surf. Coat. Technol., 2003, **174**, 193-196.

[38] X. Liu, L. Pan, Q. Zhao, T. Lv, G. Zhu, T. Chen, T. Lu, Z. Sun, C. Sun, UV-assistedphotocatalytic synthesis of ZnO–reduced graphene oxide composites with enhancedphotocatalytic activity in reduction of Cr(VI), Chemical Engineering Journal, 2012, **183**, 238-243.

[39] D. Li, H. Haneda, Morphologies of zinc oxide particles and their effects on photocatalysis,Chemosphere, 2003, **51**, 129-137.